nature chemistry

ARTICLES

https://doi.org/10.1038/s41557-022-00895-3

Stereocontrolled 1,3-nitrogen migration to access chiral α-amino acids

Chen-Xi Ye[1,3], Xiang Shen[1,3], Shuming Chen[2]✉ and Eric Meggers[1]✉

α-Amino acids are essential for life as building blocks of proteins and components of diverse natural molecules. In both industry and academia, the incorporation of unnatural amino acids is often desirable for modulating chemical, physical and pharmaceutical properties. Here we report a protocol for the economical and practical synthesis of optically active α-amino acids based on an unprecedented stereocontrolled 1,3-nitrogen shift. Our method employs abundant and easily accessible carboxylic acids as starting materials, which are first connected to a nitrogenation reagent, followed by a highly regio- and enantioselective ruthenium- or iron-catalysed C(sp^3)–H amination. This straightforward method displays a very broad scope, providing rapid access to optically active α-amino acids with aryl, allyl, propargyl and alkyl side chains, and also permits stereocontrolled late-stage amination of carboxylic-acid-containing drugs and natural products.

A direct and straightforward strategy for the synthesis of optically active α-amino acids is the catalytic enantioselective introduction of an amino group in the α-position of readily available carboxylic acids[1,2]. A number of methods for direct asymmetric C(sp^3)–H aminations have been reported and typically exploit the acidity of the C–H group next to a carbonyl functionality for electrophilic aminations via enolate intermediates[3–7]. However, most existing methods use aldehydes, ketones or dicarbonyl compounds as starting materials instead of more desirable but less acidic carboxylic acid derivatives. To further complicate matters, the electrophilic amination reagents employed are usually diazo compounds, which lead to amination products that cannot be easily converted to the target α-amino acids.

The insertion of nitrenes into C–H bonds provides a more tunable alternative platform for C(sp^3)–H aminations because the reactivity of nitrenes can be controlled by transition metal coordination. In addition, milder reaction conditions can often be used (Fig. 1a)[8]. Much progress has been made employing chiral transition metal catalysts for the enantioselective conversion of prochiral C(sp^3)–H bonds into C–N bonds by nitrene insertion[9,10]. However, intermolecular nitrene insertion reactions suffer from problems with regioselectivity and enantioselectivity (Fig. 1b)[11–19]. Although this is not the case for intramolecular C(sp^3)–H amination reactions, in which well-defined intramolecular cyclic transition states allow exquisite regio- and stereocontrol, such intramolecular C–H nitrene insertions are typically ring-closing reactions and therefore lack general applicability[20–26]. Thus, the catalytic enantioselective synthesis of acyclic amines by catalytic enantioselective C(sp^3)–H nitrene insertion remains a challenge, and its application to the synthesis of chiral α-amino acids would be highly desirable.

In this article we introduce a strategy that combines the advantages of intramolecular (regio- and stereocontrol via intramolecular cyclic transition state) and intermolecular C–H nitrene insertion chemistry (more general, acyclic products) by covalently connecting a nitrene precursor to a carboxylic acid functionality. After O–N bond cleavage and binding of both fragments to the catalyst, an intramolecular cyclic transition state facilitates a stereocontrolled C(sp^3)–H amination (Fig. 1c). This reaction constitutes an unprecedented stereocontrolled 1,3-migratory nitrene C–H insertion and is applied to the catalytic asymmetric synthesis of α-amino acids.

Results and discussion

Initial experiments and optimization. We commenced our study with carboxylic acid derivatives **1a–e** in which the nitrogen bears different electron-withdrawing protecting groups, which is established to be beneficial for generating electrophilic nitrene intermediates. The catalysts tested were 'chiral-at-metal' ruthenium complexes in which two bidentate *N*-(2-pyridyl)-substituted *N*-heterocyclic carbenes and two acetonitrile ligands are coordinated to a central ruthenium in a C_2-symmetric fashion (Table 1)[27]. Despite all ligands being achiral, the overall chirality required for asymmetric catalysis originates from a stereogenic ruthenium centre with Λ or Δ configuration, resulting in a left-handed or right-handed helical topology, respectively. We have previously demonstrated such complexes to be capable of catalysing enantioselective ring-closing C–H aminations[28,29]. Importantly, catalysts of this class feature two vacant coordination sites adjacent to each other (coordination sites of the two labile acetonitrile, highlighted in red), which is essential for the envisioned mechanistic design.

We first subjected the trifluoroacetamide substrate **1a** to the ruthenium complex Λ-**RuDMP**[27] (1 mol%) in CH_2Cl_2 in the presence of the base K_2CO_3 (3 equiv.) at room temperature (25 °C) for 16 h, but were disappointed that no conversion occurred (Table 1, entry 1). Upon replacement of the trifluoroacetamide group with a *p*-toluenesulfonyl (Ts) group (**1b**), a 37% conversion was observed, although the undesired phenylacetic acid (**PAA**) was obtained as the main product in 23% yield as measured by ^{1}H NMR (entry 2). Encouragingly, the amination product **2b** was also detected, albeit only in small quantities (<5%). A methylsulfonyl (Ms) group did not provide appreciably better results with product **2c** formed in trace amounts (<5%) (entry 3). Because of the difficulties associated with cleaving sulfonylamides, sulfonyl groups are synthetically undesirable as amine protecting groups. We therefore tested the more practical methoxycarbonyl protecting group and were delighted to find that the substrate **1d** was completely consumed under our

[1]Fachbereich Chemie, Philipps-Universität Marburg, Marburg, Germany. [2]Department of Chemistry and Biochemistry, Oberlin College, Oberlin, OH, USA. [3]These authors contributed equally: Chen-Xi Ye, Xiang Shen. ✉e-mail: shuming.chen@oberlin.edu; meggers@chemie.uni-marburg.de

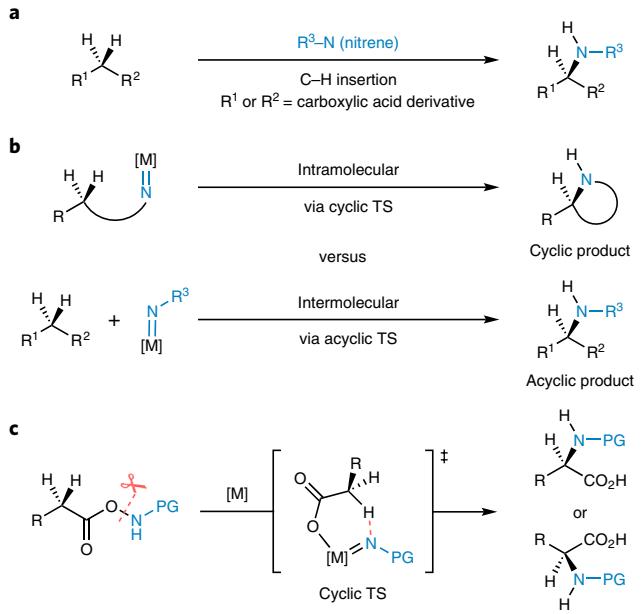

Fig. 1 | Stereocontrolled nitrene C(sp^3)–H insertions for the synthesis of α-amino acids. a, Strategy for the straightforward synthesis of α-amino acids by nitrene C–H insertion. **b**, Intramolecular nitrene C–H insertion proceeds via a cyclic transition state to form a cyclic product, while intermolecular nitrene C–H insertion forms acyclic products. **c**, Proposed 1,3-nitrogen migration which combines the advantages of intramolecular (high regio- and stereocontrol via cyclic TS) and intermolecular (acyclic product formation) C–H insertion chemistry. TS, transition state; PG, protecting group; [M], transition metal catalyst.

standard conditions and the chiral amino acid (*R*)-**2d** formed in 86% yield with 89% enantiomeric excess (e.e.) (entry 4). Finally, the best results were obtained with the 2,2,2-trichloroethoxycarbonyl (Troc) protecting group (**1e**), which provided the amino acid (*R*)-**2e** in an excellent 93% yield as determined by ^{1}H NMR and with 95% e.e. (entry 5). Other catalysts with different substituents on the pyridine moieties provided inferior results; replacing the 3,5-dimethylphenyl groups with trimethylsilyl (TMS) groups (Λ-**RuTMS** (ref. [28])), CF_3 groups (Λ-**RuCF$_3$** (ref. [29])) or just hydrogen (Λ-**RuH** (ref. [27])) resulted in reduced yields and enantioselectivities (entries 6–8). Table 1 also reveals that CH_2Cl_2 is the optimal solvent and K_2CO_3 the optimal base for this stereocontrolled 1,3-nitrogen shift (entries 9–12 and Supplementary Table 1).

Substrate scope for ruthenium catalysis. With the optimal reaction conditions in hand, we investigated the scope of this stereocontrolled 1,3-nitrogen shift. *N*,*N*′-Dicyclohexylcarbodiimide (DCC)- or 1-ethyl-3-(3-dimethylaminopropyl)carbodiimide hydrochloride (EDCI)-induced coupling of readily available carboxylic acids with *N*-Troc-protected hydroxylamine provided rapid access to a variety of azanyl esters, which were then subjected to the rearrangement under the developed standard conditions (Table 2). We started with functionalizing the phenyl moiety of phenylacetic acid azanyl ester **1e** and found that the method tolerates a large variety of different substituents in the phenyl ring, affording the corresponding chiral α-amino acids **3**–**21** in up to 96% yield and with up to 98% e.e. Electron-donating functional groups in the phenyl moiety such as methyl (α-amino acid **3**), methoxy (α-amino acids **5**), 1,3-dioxole (α-amino acid **8**), a Fmoc-protected alcohol (α-amino acid **9**), hydroxymethyl (α-amino acid **10**) and *N*-pivaloylamide (α-amino acid **19**) are tolerated, as are electron-withdrawing substituents such as halogens (α-amino acids **11**–**14**), trifluoromethyl (α-amino acid **15**), nitro (α-amino acid **16**), acetyl (α-amino acid **17**) and methoxycarbonyl (α-amino acid **18**). The method also enables the synthesis of the azido α-amino acid **20** (95% yield and 97% e.e.) and the alkynyl α-amino acid **21** (88% yield, 94% e.e.), both of which are building blocks of interest for click chemistry (see Supplementary Table 2 regarding the configurational stability of the generated stereocentre)[30]. The stereocontrolled 1,3-nitrogen shift was also applied to the synthesis of α-aryl amino acids with benzannulated aromatic and heteroaromatic systems (α-amino acids **22**–**25**) in 77–92% yield and with 90–96% e.e. Notably, the reaction could be readily scaled up to afford the naphthyl α-amino acid **23** in gram quantities with high yield (91%) and enantiopurity (95% e.e., increased to 99% e.e. after crystallization protocol, see Supplementary Fig. 1). It is noteworthy that the stereocontrolled 1,3-nitrogen shift can also be applied to the late-stage functionalization of bioactive compounds. For example, isoxepac[31] is an arylacetic acid derivative with anti-inflammatory and analgesic activity, the azanyl ester of which was converted to the corresponding α-amino acid **26** in 87% yield and with 98% e.e. Diclofenac[32], a pain medication for the treatment of inflammatory diseases, was converted into its azanyl ester and then rearranged to afford α-amino acid **27** in 54% yield and with 96% e.e., which is remarkable considering the presence of an unprotected and sterically hindered aniline moiety in the *ortho*-position.

We also investigated C–H aminations at non-benzylic positions and discovered that the stereocontrolled 1,3-nitrogen shift can be applied to the asymmetric synthesis of chiral α-amino acids with alkenyl (**28**–**32**) and alkynyl (**34** and **35**) side chains, albeit with somewhat reduced enantioselectivities (62–84% e.e.). Even the unusual Troc-protected 2-amino-(*E*)-3,5-hexadienoic acid (**33**) could be synthesized in 72% yield and with 81% e.e. These results show that the stereocontrolled 1,3-nitrogen shift is applicable to benzylic, allylic and propargylic C–H bonds. However, the application of this shift to completely non-activated aliphatic methylene groups provides inferior results, with the α-amino acid **36** obtained in merely 20% yield, albeit with a satisfactory 90% e.e.

Next, we investigated the asymmetric synthesis of α-disubstituted α-amino acids by amination of tertiary C–H bonds at a stereogenic carbon centre. When we reacted racemic azanyl ester **37** under our standard conditions, the corresponding 2-amino-2-phenylpropanoic acid (*R*)-**38** was obtained in 71% yield but with a modest 48% e.e. Since the azanyl ester is chiral, we expected high stereodiscrimination between enantiotopic C–H bonds. Indeed, the *S*-enantiomer (*S*)-**37** (99% e.e.) afforded the α-amino acid (*R*)-**38** smoothly in 91% yield and with 98% e.e. (matched substrate/catalyst combination) while the mirror-imaged substrate (*R*)-**37** reacted sluggishly, providing the α-amino acid (*S*)-**38** in 34% yield with 28% e.e. (mismatched substrate/catalyst combination). The stereospecific C–H amination of chiral non-racemic substrates is general and was applied to the synthesis of the α-disubstituted α-amino acids **39**–**42** in 25–86% yield and with 86–99% e.e. For example, the azanyl ester of the non-steroidal anti-inflammatory drug naproxen, which contains an *S*-configured stereocentre, was converted to the corresponding α-amino acid **39** in 86% yield and 99% e.e., with virtually complete stereoretention. The C–H amination is also applicable to completely non-activated tertiary C(sp^3)–H bonds, as demonstrated by α-amino acids **41** and **42**.

Substrate scope for iron catalysis. To expand the substrate scope, we turned our attention to iron catalysis[33], which has additional economic and environmental benefits. Iron-catalysed C–H bond aminations through nitrenoid intermediates have been reported, including the (racemic) amination of non-activated aliphatic C(sp^3)–H bonds[34]. We utilized the conversion of azanyl ester **1e** to the *N*-Troc-protected phenylglycine **2e** as the initial model reaction to identify a suitable iron catalyst (Table 3).

Table 1 | Initial experiments and optimization of enantioselective 1,3-nitrogen shift

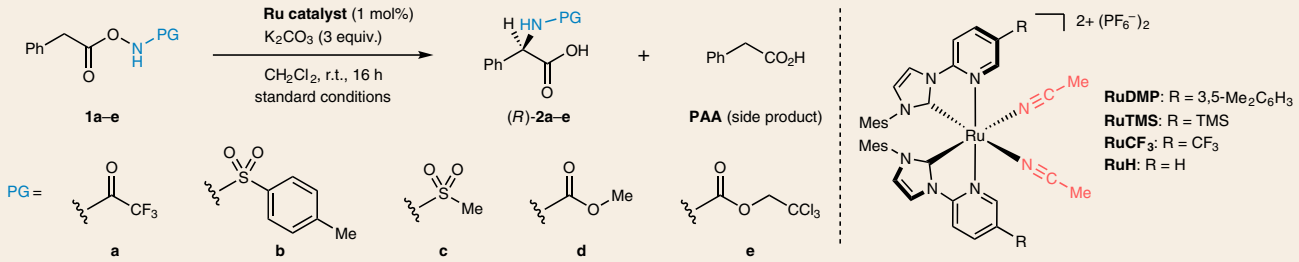

Entry	Catalyst	Protecting group (PG)	Conditions[a]	Conversion (%)[b]	Yield of 2 (%)[b]	Yield of PAA (%)[b]	e.e. of 2 (%)[c]
1	Λ-**RuDMP**	$COCF_3$ (**a**)	Standard	0	–	–	–
2	Λ-**RuDMP**	Ts (**b**)	Standard	37	<5	23	n.d.
3	Λ-**RuDMP**	Ms (**c**)	Standard	50	<5	25	n.d.
4	Λ-**RuDMP**	CO_2Me (**d**)	Standard	100	86	12	89
5	Λ-**RuDMP**	Troc (**e**)	Standard	100	93 (91)[d]	4	95
6	Λ-**RuTMS**	Troc (**e**)	Standard	98	80	9	92
7	Λ-**RuCF$_3$**	Troc (**e**)	Standard	19	6	5	90
8	Λ-**RuH**	Troc (**e**)	Standard	100	85	9	92
9	Λ-**RuDMP**	Troc (**e**)	Et_3N as base	100	25	73	95
10	Λ-**RuDMP**	Troc (**e**)	Na_2CO_3 as base	99	87	5	95
11	Λ-**RuDMP**	Troc (**e**)	THF as solvent	94	15	75	82
12	Λ-**RuDMP**	Troc (**e**)	MeOH as solvent	96	0	64	–

[a]Shown are the deviations from the standard reaction conditions. Standard conditions: substrate **1** (0.1 mmol), ruthenium catalyst (1 mol%) and the indicated base (3 equiv.) in the indicated solvent (2 ml, 0.05 M) were stirred at room temperature (25 °C) for 16 h. [b]Conversion and yield were determined by ^{1}H NMR analysis using hexamethylbenzene as an internal standard. [c]Enantiomeric excess (e.e.) values were determined by HPLC on chiral stationary phases. [d]Yield of the isolated α-amino acid. n.d., not determined; Troc, $CO_2CH_2CCl_3$.

The chiral-at-iron complex Δ-**Fe1** (ref. [35]), a lighter homologue of the chiral-at-ruthenium complexes used in this study, provided disappointing results with only trace amounts of product. We next investigated non-haem iron complexes with linear tetradentate *N*4-donor ligands coordinated in a *cis*-α-topological configuration. The overall helical topology is similar to that of the ruthenium catalysts, including the presence of two adjacent labile ligands. Using bis-pyridine complexes (*R*,*R*)-**Fe2** and (*R*,*R*)-**Fe3** featuring a rigid chiral 2,2′-bipyrrolidine backbone[36,37], we obtained the desired amino acid (*S*)-**2e** in 91% and 75% yield, respectively, albeit with <20% e.e. Fortunately, replacing the pyridyl moieties with *N*-methylbenzimidazole[38] (**BIP** ligand) and using labile chloride ligands instead of acetonitrile resulted in the air- and moisture-stable neutral complex (*R*,*R*)-[$FeCl_2$(**BIP**)] ((*R*,*R*)-**FeBIP**), which provided phenylglycine (*S*)-**2e** in 95% yield and with a satisfactory 91% e.e. While the amination of benzylic (**2e**), allylic (**32**) and propargylic (**34**) positions cannot compete with the results obtained for ruthenium catalysis, we found that (*R*,*R*)-**FeBIP** is a superior catalyst for the generation of non-racemic α-amino acids with non-activating aliphatic side chains. Substrates with primary (**43**–**50**), secondary (**51**) and tertiary (**36**) aliphatic side chains underwent amination in 48–75% yield and with 85–92% e.e. The method is also suitable for the late-stage amination of more complex molecules. Azanyl ester formation followed by iron-catalysed stereocontrolled 1,3-nitrogen shift converted lithocholic acid to amino acid **52** (77% yield, 23:1 d.r.). The iron-catalysed protocol can also be used for the amination of tertiary C(sp^3)–H bonds as shown for racemic ibuprofen, which was converted to amino acid **53** in 70% yield and with 85% e.e. in a stereoconvergent transformation.

Mechanistic investigations. We performed density functional theory (DFT) calculations to elucidate the reaction mechanism and provide deeper insight (Fig. 2a). Ruthenium catalyst **RuH** and the methylcarbamate substrate **1d** were used as the model system. Because the catalyst contains two adjacent labile MeCN ligands and the azanyl ester substrate several suitable coordination sites, it is reasonable to expect that the mechanism proceeds through an initial bidentate coordination. Indeed, the DFT calculations are consistent with this picture. Stepwise displacement of two labile acetonitrile ligands from the ruthenium centre of **RuH** by substrate **1d** gives rise to intermediate **I**, which proceeds to the chelate coordination mode **II** with a modest 6.2 kcal mol^{-1} increase in free energy. The amide N–H bond in **II** is now sufficiently acidified to be deprotonated by a weak base such as trimethylamine, leading to the deprotonated chelate intermediate **III**. A subsequent N–O cleavage occurs through the cyclic transition state **TS-I** with a free energy barrier of 13.6 kcal mol^{-1} to yield ruthenium nitrene **IV** in an exergonic fashion. Although the singlet nitrene complex ^{1}**IV** is calculated to be 2.3 kcal mol^{-1} more stable than the triplet nitrene complex ^{3}**IV**, the C–H cleavage transition state **TS-II** is lower in energy in the triplet state (^{3}**TS-II** versus ^{1}**TS-II**). This indicates the possibility of a Curtin–Hammett situation in which the presence of the late transition metal ruthenium enhances rapid singlet–triplet spin crossover[39–41], followed by a preferred exergonic hydrogen atom transfer (HAT) from ^{3}**IV** through the cyclic transition state ^{3}**TS-II** to afford the diradical ^{3}**V**. Facile intersystem crossing between intersecting singlet and triplet energy surfaces has also been implicated in other systems involving nitrenoid intermediates, such as copper- and silver-catalysed olefin aziridinations[42] and C(sp^3)–H amidations promoted by a ruthenium photocatalyst[43]. An experimentally determined kinetic isotope effect value of $k_H/k_D = 2.9$ indicates that this homolytic C–H cleavage occurs during the rate-determining step and is consistent with the calculated free energy barrier of 13.9 kcal for the HAT step on the triplet energy surface. A radical mechanism is also supported by an observed $Z \rightarrow E$ alkene isomerization in an allylic C–H amination reaction (see Supplementary Fig. 2 for these mechanistic experiments). Taken together, these computational

Table 2 | Substrate scope for ruthenium catalysis

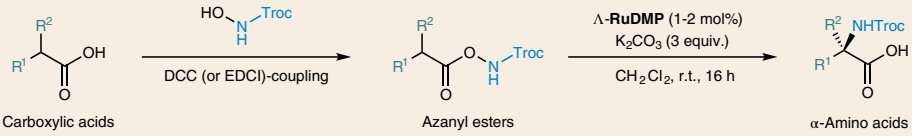

α-Aryl amino acids

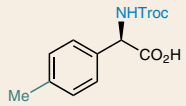

3
86%, 97% e.e.

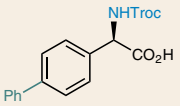

4
86%, 95% e.e.

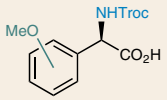

5 (*para*), 96%, 96% e.e.
6 (*meta*), 87%, 96% e.e.
7 (*ortho*), 79%, 85% e.e.

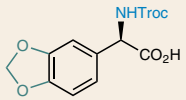

8
56%, 92% e.e.

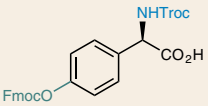

9
83%, 93% e.e.

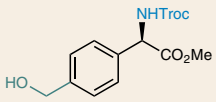

10[a]
64%, 98% e.e.

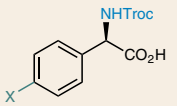

11, X = I, 91%, 94% e.e.
12, X = Br, 93%, 94% e.e
13, X = Cl, 93%, 95% e.e.
14, X = F, 92%, 93% e.e.

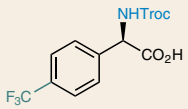

15
87%, 86% e.e.

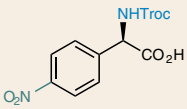

16
73%, 92% e.e.

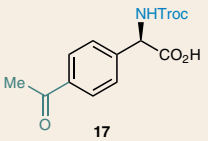

17
79%, 92% e.e.

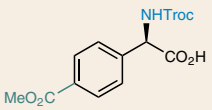

18
91%, 93% e.e.

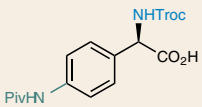

19
93%, 96% e.e.

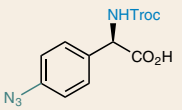

20
95%, 97% e.e.

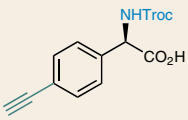

21
88%, 94% e.e.

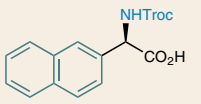

22
92%, 96% e.e.

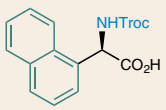

23[b]
92%, 95% e.e.

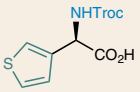

24
84%, 95% e.e.

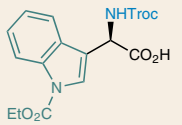

25
77%, 90% e.e.

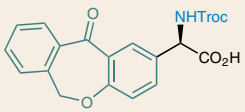

26 (87%, 98% e.e.)
from isoxepac

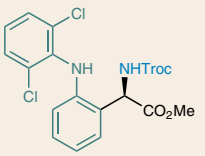

27[a] (54%, 96% e.e.)
from diclofenac

α-Alkenyl, α-alkynyl and α-alkyl amino acids

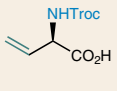

28
62%, 73% e.e.

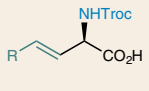

29, R = Et, 83%, 84% e.e.
30, R = ^{i}Pr, 88%, 81% e.e.
31, R = ^{n}Hex, 85%, 82% e.e.
32, R = Ph, 88%, 82% e.e.

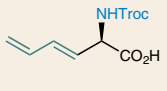

33
72%, 81% e.e.

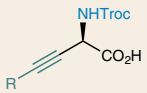

34[c], R = Ph, 46%, 62% e.e.
35[c], R = Et, 63%, 64% e.e.

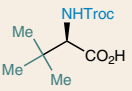

36[d]
20%, 90% e.e.

α-Disubstituted amino acids (stereoretentive 1,3-nitrogen shift)

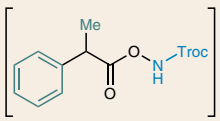

Azanyl ester **37**

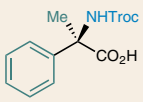

(*R*)-**38**[e]
91%, 98% e.e.[f]

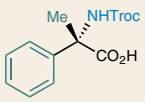

(*S*)-**38**[g]
34%, 28% e.e.

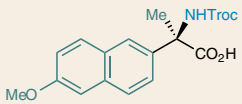

39[f] (86%, 99% e.e.)
from naproxen

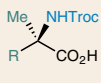

40[d,f], R = (*E*)-EtCH=CH, 77%, 87% e.e.
41[d,f], R = Et, 57%, 86% e.e.
42[d,f], R = cyclohexyl, 25%, 92% e.e.

Conditions for enantioselective 1,3-nitrogen shift: reactions were carried out with Λ-**RuDMP** (1–2 mol%), K_2CO_3 (3 equiv.) and CH_2Cl_2 (0.05 M) at room temperature (25 °C) for 16 h. Enantiomeric excess (e.e.) values were determined by HPLC analysis (see Supplementary Information section 4 for full details). [a]Isolated after conversion to the methyl ester. [b]Additional gram-scale reaction performed with 3.5 mmol (1.32 g) azanyl ester gave **23** in 91% yield with 95% e.e. (see Supplementary Information section 6 for full details). [c]$KHCO_3$ instead of K_2CO_3 as a base. [d]Λ-**RuH** (2–10 mol%) as the catalyst. [e]The reaction performed with racemic azanyl ester **37** afforded (*R*)-**38** in 71% yield with 48% e.e. [f]Reaction performed with enantiopure (*S*)-azanyl ester. [g]Reaction performed with enantiopure (*R*)-azanyl ester.

and experimental results indicate that the dominant mechanistic C–H cleavage pathway involves triplet HAT, not concerted singlet nitrene insertion. Calculated spin densities of the intermediate ^{3}**V**, formed in the course of the HAT, indicate that the singly occupied molecular orbitals are mostly located on the ruthenium centre and the α-carbon of the coordinated substrate so that intermediate ^{3}**V** is best represented as a triplet diradical (see framed structure of ^{3}**V** in Fig. 2a). Intermediate ^{3}**V** undergoes a strongly exergonic radical recombination to form ^{1}**VI** upon spin crossover to the singlet state through a minimum-energy crossing point. Subsequent O-protonation and release of product **2d** then completes the catalytic cycle.

Table 3 | Substrate scope for iron catalysis

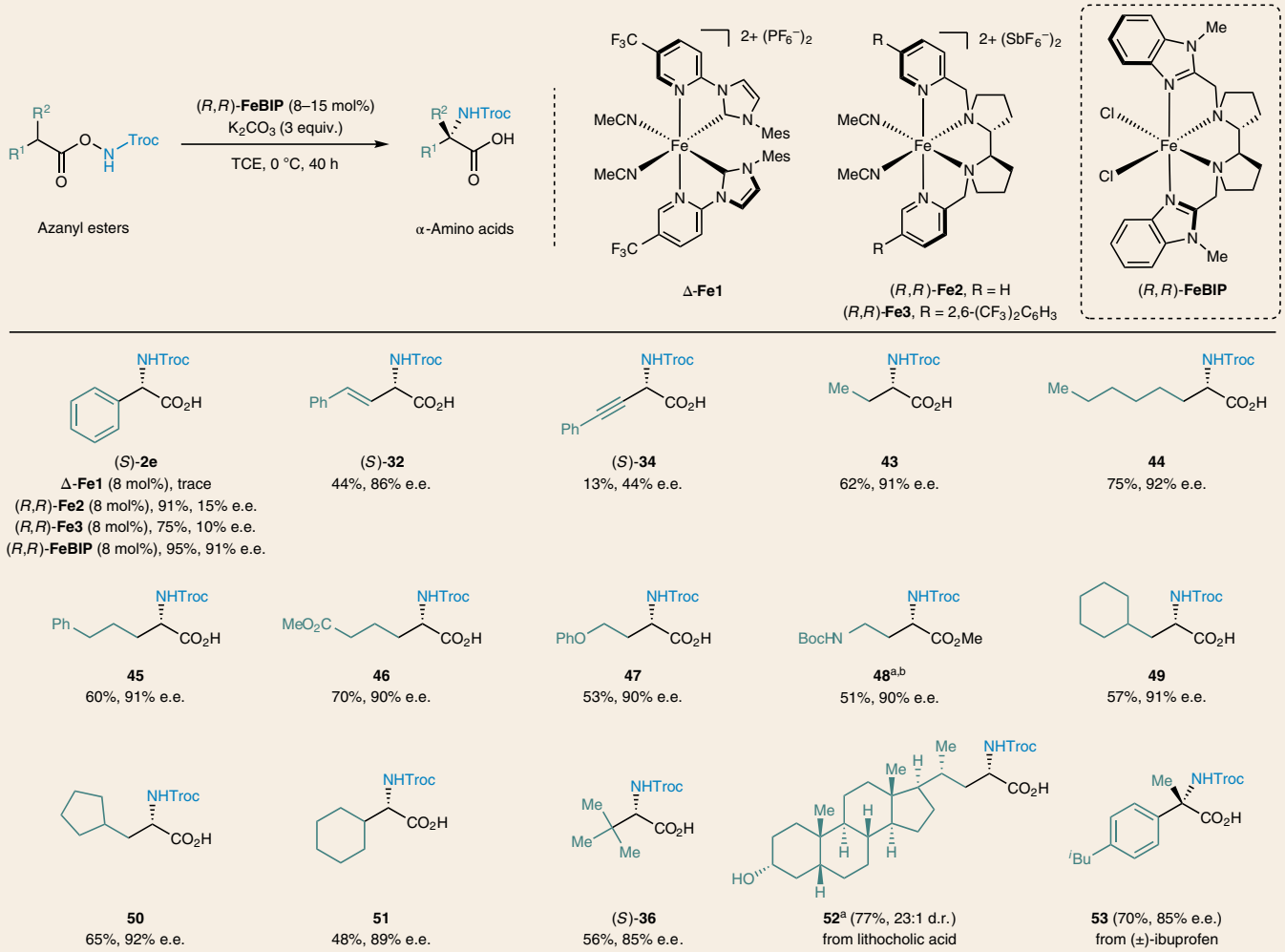

Reaction conditions: reactions were carried out with (*R*,*R*)-**FeBIP** (8–15 mol%), K_2CO_3 (3 equiv.) and 1,1,2,2-tetrachloroethane (TCE, 0.1 M) at 0 °C for 40 h. Enantiomeric excess (e.e.) values were determined by HPLC analysis (see Supplementary Information section 4 for full details). [a]Reaction performed at room temperature (25 °C) for 16 h. [b]Isolated after conversion to the methyl ester. d.r., diastereomeric ratio.

Our calculations also provide insight into the origins of stereocontrol in the 1,3-nitrogen shift. Figure 2b shows the geometries of the calculated cyclic transition state for the HAT step involving the model substrate **1d** bearing a phenyl substituent. Non-covalent interaction plots reveal that the transition state leading to the experimentally observed major product enantiomer, **^{3}TS-II-major-Ph**, is stabilized by a π–π stacking interaction between a pyridine ligand of the catalyst and the phenyl substituent on the substrate. This π–π stacking interaction is absent from the disfavoured minor transition state **^{3}TS-II-minor-Ph**, which is 1.5 kcal mol^{-1} higher in energy than **^{3}TS-II-major-Ph**. When implicit CH_2Cl_2 solvent was incorporated in the TS geometry optimizations (see Supplementary Information, sections 8.4–8.6), the free energy difference was found to be 2.1 kcal mol^{-1}, favouring **^{3}TS-II-major-Ph**, consistent with the calculations in the gas phase. Following the stereoselective HAT, the resulting diradical **V** presumably undergoes spin crossover and recombination faster than C–C bond rotation, allowing the stereoselectivity of the HAT step to be preserved in the nitrogenated product. This is consistent with the C–H amination of chiral substrates such as (*S*)-**37**, in which the C–H bond is converted to a C–N bond under retention of configuration. Distortion–interaction analysis[44] performed on the two transition states indicates that the distortion energies are 1.4 kcal mol^{-1} lower for **^{3}TS-II-minor-Ph**, but the interaction energy is 2.9 kcal mol^{-1} more favourable in **^{3}TS-II-major-Ph** (Fig. 2c). These results provide further support that stabilizing interactions such as π–π stacking contribute to the observed stereoselectivity in the formation of phenylglycine derivative **2d**. However, our calculations confirm that stereodiscrimination can also be achieved in the absence of attractive π–π stacking interactions as demonstrated for a substrate bearing a *tert*-butyl instead of a phenyl side chain, which is consistent with the experimental results (for example, formation of amino acid **36**). The transition state producing the major product enantiomer, **^{3}TS-II-major-^{t}Bu**, was calculated to be 1.3 kcal mol^{-1} more favourable than **^{3}TS-II-minor-^{t}Bu**. This result is in good agreement with the experimentally observed 90% e.e. value. In **^{3}TS-II-minor-^{t}Bu**, the *tert*-butyl substituent of the coordinated carboxylate sterically clashes with the acyl Ru-nitrenoid fragment, creating destabilizing close contacts that are absent from **^{3}TS-II-major-^{t}Bu**. Such destabilizing close contacts are also absent from the transition states with the phenyl side chain. Taken together, these results support the conclusion that effective stereodiscrimination can either be achieved through π–π stacking (in the case of Ph side chain) or steric effects (in the case of ^{t}Bu side chain), although contributions from additional attractive interactions, such as C–H···π interactions, cannot be ruled out in **^{3}TS-II-major-^{t}Bu** (refs. [45–47]).

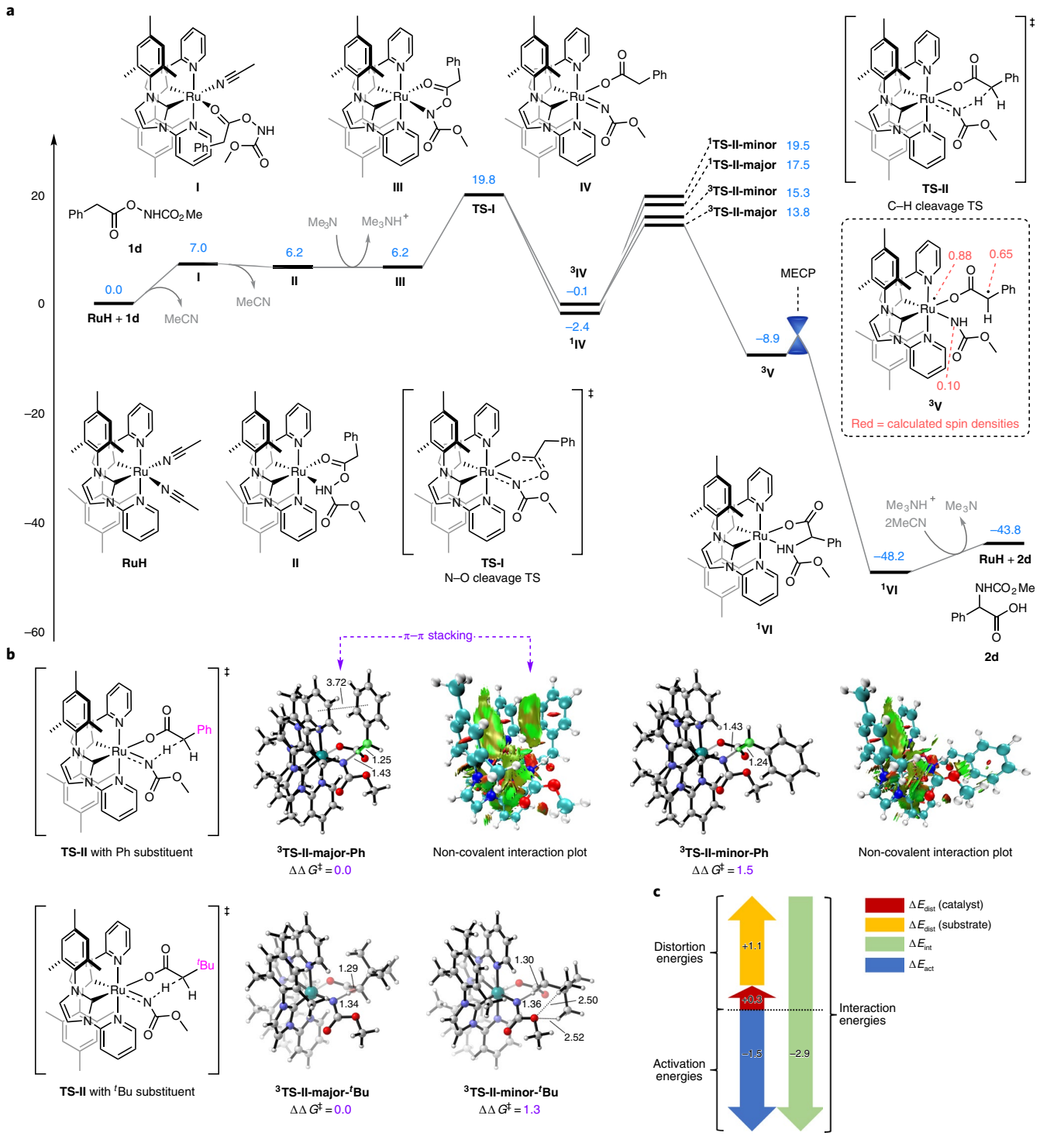

Fig. 2 | Investigation of the reaction mechanism. a, Calculated free-energy profile for the 1,3-nitrogen migration of model substrate **1d** with **RuH** as the catalyst (energies provided in kcal mol^{-1}). Ruthenium catalyses the cleavage of the N–O bond of **1d** via transition state **TS-I**, leading to the carboxylate-coordinated ruthenium nitrene intermediate **IV**. This is followed by singlet–triplet spin crossover to the triplet state of **IV** followed by an exergonic hydrogen atom transfer via cyclic transition state **TS-II** to generate diradical intermediate **V** in its triplet state. Next, C–N bond formation occurs upon spin crossover to the singlet state through a minimum-energy crossing point (MECP) to generate the chelate complex **VI**. Protonation of the coordinated carboxylate moiety finally releases the product **2d**. **b**, Geometries and non-covalent interaction plots of calculated transition states for the hydrogen atom transfer step to provide insight into the origin of stereodiscrimination (interatomic distances provided in ångströms). The results reveal that in **^{3}TS-II-major-Ph** (color code: C, grey; H, white; N, blue; O, red; Ru, turquoise; to be cleaved C-H bond highlighted in green), a favourable π–π stacking interaction exists between the ligand framework of the catalyst and the phenyl substituent of the substrate **1d** (**TS-II** with Ph substituent). This favourable π–π stacking interaction is absent from **^{3}TS-II-minor-Ph**. The calculations also confirm that stereodiscrimination can be achieved with a substrate bearing a ^{t}Bu instead of a Ph side chain (**TS-II** with ^{t}Bu substituent). **c**, Distortion–interaction analysis performed on **^{3}TS-II-major-Ph** and **^{3}TS-II-minor-Ph**. The more favourable interaction energy in **^{3}TS-II-major-Ph** further supports the contribution of stabilizing interactions such as π–π stacking to the stereoselectivity in the formation of phenylglycine derivative **2d**.

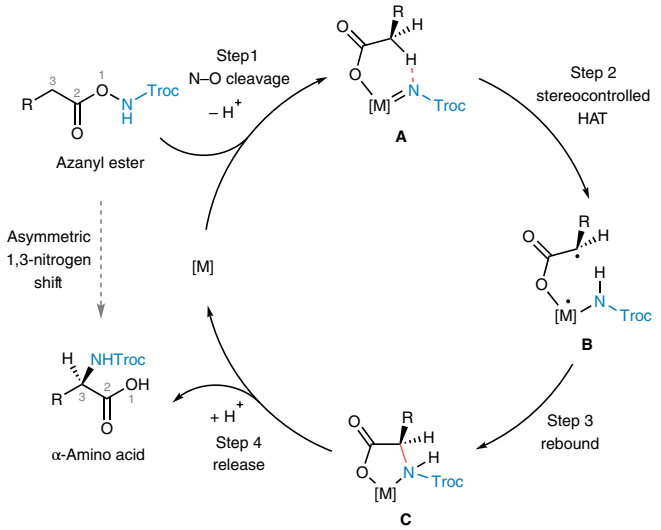

Fig. 3 | Summary of proposed simplified mechanism. The catalytic cycle of the asymmetric 1,3-nitrogen migration commences with N–O cleavage of azanyl ester in the presence of metal catalyst, proceeds through stereocontrolled hydrogen atom transfer and subsequent rebound of the diradical, and concludes with release of the α-amino acid and catalyst regeneration.

A simplified mechanism based on the DFT calculations and control experiments discussed above is shown Fig. 3. The azanyl ester substrate is first activated by N–O cleavage to provide intermediate **A** (corresponding to intermediate **IV** in Fig. 2a) after deprotonation. A subsequent stereocontrolled HAT then affords the diradical **B** (corresponding to intermediate **V** in Fig. 2a), followed by a rapid radical rebound to yield the chelate complex **C** (corresponding to intermediate **VI** in Fig. 2a). Protonation of the carboxylate induces product dissociation and concludes the catalytic cycle. The net result of the N–O bond fragmentation and subsequent stepwise C–H insertion is an asymmetric 1,3-nitrogen shift to provide non-racemic chiral α-amino acids.

Conclusions

We report the catalytic enantioselective synthesis of chiral α-amino acids by an enantioselective 1,3-migratory nitrene C(sp^3)–H insertion. The method is based on a unique stereocontrolled 1,3-nitrogen shift from one carboxylic acid oxygen to the α-carbon. Our method employs abundant and easily accessible carboxylic acids as starting materials. Ligation to a nitrene precursor, followed by intramolecular C–H cleavage through an intramolecular cyclic transition state, ensures high regio- and stereocontrol in the synthesis of non-racemic chiral α-amino acids. Chiral ruthenium and iron catalysis jointly provide a very broad scope, enabling rapid access to optically active α-amino acids with aryl, allyl, propargyl (ruthenium catalysis) and non-activated alkyl (iron catalysis) side chains, including α-disubstituted amino acids by stereoretentive (ruthenium catalysis) or enantioconvergent (iron catalysis) C–H amination. The high functional group tolerance of this method also permits the enantioselective late-stage amination of carboxylic-acid-containing drugs and natural products. The Troc-protected amino acids obtained through this protocol can be used directly in synthesis with the Troc group being selectively removable under mild conditions via a reductive Grob fragmentation[48]. This strategy will expedite the synthesis of unnatural α-amino acids, which are important building blocks of peptidomimetic drugs, as well as engineered proteins and enzymes with modulated properties[49–51].

Online content

Any methods, additional references, Nature Research reporting summaries, source data, extended data, supplementary information, acknowledgements, peer review information; details of author contributions and competing interests; and statements of data and code availability are available at https://doi.org/10.1038/s41557-022-00895-3.

Received: 14 March 2021; Accepted: 19 January 2022;
Published online: 04 April 2022

References

1. Saghyan, A. S. & Langer, P. *Asymmetric Synthesis of Non-proteinogenic Amino Acids* (Wiley-VCH, 2016).
2. Nájera, C. & Sansano, J. M. Catalytic asymmetric synthesis of α-amino acids. *Chem. Rev.* **107**, 4584–4671 (2007).
3. Janey, J. M. Recent advances in catalytic, enantioselective α aminations and α oxygenations of carbonyl compounds. *Angew. Chem. Int. Ed.* **44**, 4292–4300 (2005).
4. Bøgevig, A., Juhl, K., Kumaragurubaran, N., Zhuang, W. & Jørgensen, K. A. Direct organo-catalytic asymmetric α-amination of aldehydes—a simple approach to optically active α-amino aldehydes, α-amino alcohols, and α-amino acids. *Angew. Chem. Int. Ed.* **41**, 1790–1793 (2002).
5. List, B. Direct catalytic asymmetric α-amination of aldehydes. *J. Am. Chem. Soc.* **124**, 5656–5657 (2002).
6. Kumaragurubaran, N., Juhl, K., Zhuang, W., Bøgevig, A. & Jørgensen, K. A. Direct L-proline-catalyzed asymmetric α-amination of ketones. *J. Am. Chem. Soc.* **124**, 6254–6255 (2002).
7. Morrill, L. C., Lebl, T., Slawin, A. M. Z. & Smith, A. D. Catalytic asymmetric α-amination of carboxylic acids using isothioureas. *Chem. Sci.* **3**, 2088–2093 (2012).
8. Dequirez, G., Pons, V. & Dauban, P. Nitrene chemistry in organic synthesis: still in its infancy? *Angew. Chem. Int. Ed.* **51**, 7384–7395 (2012).
9. Park, Y., Kim, Y. & Chang, S. Transition metal-catalyzed C–H amination: scope, mechanism, and applications. *Chem. Rev.* **117**, 9247–9301 (2017).
10. Ju, M. & Schomaker, J. M. Nitrene transfer catalysts for enantioselective C–N bond formation. *Nat. Rev. Chem.* **5**, 580–594 (2021).
11. Nägeli, I. et al. Rhodium(II)-catalyzed CH insertions with {[(4-nitrophenyl) sulfonyl]imino}phenyl-λ3-iodane. *Helv. Chim. Acta* **80**, 1087–1105 (1997).
12. Zhou, X.-G., Yu, X.-Q., Huang, J.-S. & Che, C.-M. Asymmetric amidation of saturated C–H bonds catalysed by chiral ruthenium and manganese porphyrins. *Chem. Commun*. 2377–2378 (1999).
13. Kohmura, Y. & Katsuki, T. Mn(salen)-catalyzed enantioselective C–H amination. *Tetrahedron Lett.* **42**, 3339–3342 (2001).
14. Yamawaki, M., Tsutsui, H., Kitagaki, S., Anada, M. & Hashimoto, S. Dirhodium(II) tetrakis[*N*-tetrachlorophthaloyl-(*S*)-tert-leucinate]: a new chiral Rh(II) catalyst for enantioselective amidation of C–H bonds. *Tetrahedron Lett.* **43**, 9561–9564 (2002).
15. Liang, C. et al. Efficient diastereoselective intermolecular rhodium-catalyzed C–H amination. *Angew. Chem. Int. Ed.* **45**, 4641–4644 (2006).
16. Nishioka, Y., Uchida, T. & Katsuki, T. Enantio- and regioselective intermolecular benzylic and allylic C–H bond amination. *Angew. Chem. Int. Ed.* **52**, 1739–1742 (2013).
17. Höke, T., Herdtweck, E. & Bach, T. Hydrogen-bond mediated regio- and enantioselectivity in a C–H amination reaction catalysed by a supramolecular Rh(II) complex. *Chem. Commun.* **49**, 8009–8011 (2013).
18. Nasrallah, A. et al. Catalytic enantioselective intermolecular benzylic C(sp^3)–H amination. *Angew. Chem. Int. Ed.* **58**, 8192–8196 (2019).
19. Jin, L.-M., Xu, P., Xie, J. & Zhang, X. P. Enantioselective intermolecular radical C–H amination. *J. Am. Chem. Soc.* **142**, 20828–20836 (2020).
20. Liang, J.-L., Yuan, S.-X., Huang, J.-S., Yu, W.-Y. & Che, C.-M. Highly diastereo- and enantioselective intramolecular amidation of saturated C–H bonds catalyzed by ruthenium porphyrins. *Angew. Chem. Int. Ed.* **41**, 3465–3468 (2002).
21. Milczek, E., Boudet, N. & Blakey, S. Enantioselective C–H amination using cationic ruthenium(II)–pybox catalysts. *Angew. Chem. Int. Ed.* **47**, 6825–6828 (2008).
22. Ichinose, M. et al. Enantioselective intramolecular benzylic C–H bond amination: efficient synthesis of optically active benzosultams. *Angew. Chem. Int. Ed.* **50**, 9884–9887 (2011).
23. Zalatan, D. N. & Du Bois, J. A chiral rhodium carboxamidate catalyst for enantioselective C–H amination. *J. Am. Chem. Soc.* **130**, 9220–9221 (2008).
24. Lang, K., Torker, S., Wojtas, L. & Zhang, X. P. Asymmetric induction and enantiodivergence in catalytic radical C–H amination via enantiodifferentiative H-atom abstraction and stereoretentive radical substitution. *J. Am. Chem. Soc.* **141**, 12388–12396 (2019).

25. Park, Y. & Chang, S. Asymmetric formation of γ-lactams via C–H amidation enabled by chiral hydrogen-bond-donor catalysts. *Nat. Catal.* **9**, 219–227 (2019).
26. van Vliet, K. M. & de Bruin, B. Dioxazolones: stable substrates for the catalytic transfer of acyl nitrenes. *ACS Catal.* **10**, 4751–4769 (2020).
27. Zheng, Y. et al. Octahedral ruthenium complex with exclusive metal-centered chirality for highly effective asymmetric catalysis. *J. Am. Chem. Soc.* **139**, 4322–4325 (2017).
28. Zhou, Z. et al. Catalytic enantioselective intramolecular C(sp^3)–H amination of 2-azidoacetamides. *Angew. Chem. Int. Ed.* **58**, 1088–1093 (2019).
29. Zhou, Z. et al. Enantioselective ring-closing C–H amination of urea derivatives. *Chem* **6**, 2024–2034 (2020).
30. Thirumurugan, P., Matosiuk, D. & Jozwiak, K. Click chemistry for drug development and diverse chemical–biology applications. *Chem. Rev.* **113**, 4905–4979 (2013).
31. Ueno, K. et al. 6,11-Dihydro-11-oxodibenz[b,e]oxepinacetic acids with potent antiinflammatory activity. *J. Med. Chem.* **19**, 941–946 (1976).
32. Krupp, P. J. et al. Sodium [*o*-[(2,6-dichlorophenyl)-amino]-phenyl]-acetate (GP 45 840), a new non-steroidal anti-inflammatory agent. *Experientia* **29**, 450–452 (1973).
33. Bauer, I. & Knölker, H.-J. Iron catalysis in organic synthesis. *Chem. Rev.* **115**, 3170–3387 (2015).
34. Liu, Y. et al. Iron- and cobalt-catalyzed C(sp^3)–H bond functionalization reactions and their application in organic synthesis. *Chem. Soc. Rev.* **49**, 5310–5358 (2020).
35. Hong, Y., Jarrige, L., Harms, K. & Meggers, E. Chiral-at-iron catalyst: expanding the chemical space for asymmetric earth-abundant metal catalysis. *J. Am. Chem. Soc.* **141**, 4569–4572 (2019).
36. Chen, M. S. & White, M. C. A predictably selective aliphatic C–H oxidation reaction for complex molecule synthesis. *Science* **318**, 783–787 (2007).
37. Gormisky, P. E. & White, M. C. Catalyst-controlled aliphatic C–H oxidations with a predictive model for site-selectivity. *J. Am. Chem. Soc.* **135**, 14052–14055 (2013).
38. Mitra, M. et al. Highly enantioselective epoxidation of olefins by H_2O_2 catalyzed by a non-heme Fe(II) catalyst of a chiral tetradentate ligand. *Dalton Trans.* **48**, 6123–6131 (2019).
39. Poli, R. & Harvey, J. N. Spin forbidden chemical reactions of transition metal compounds. New ideas and new computational challenges. *Chem. Soc. Rev.* **32**, 1–8 (2003).
40. Harvey, J. N., Poli, R. & Smith, K. M. Understanding the reactivity of transition metal complexes involving multiple spin states. *Coord. Chem. Rev.* **238-239**, 347–361 (2003).
41. Yersin, H. & Humbs, W. Spatial extensions of excited states of metal complexes. Tunability by chemical variation. *Inorg. Chem.* **38**, 5820–5831 (1999).
42. Maestre, L., Sameera, W. M. C., Díaz-Requejo, M. M., Maseras, F. & Pérez, P. J. A general mechanism for the copper- and silver-catalyzed olefin aziridination reactions: concomitant involvement of the singlet and triplet pathways. *J. Am. Chem. Soc.* **135**, 1338–1348 (2013).
43. Jung, H., Keum, H., Kweon, J. & Chang, S. Tuning triplet energy transfer of hydroxamates as the nitrene precursor for intramolecular C(sp^3)–H amidation. *J. Am. Chem. Soc.* **142**, 5811–5818 (2020).
44. Ess, D. H. & Houk, K. N. Theory of 1,3-dipolar cycloadditions: distortion/interaction and frontier molecular orbital models. *J. Am. Chem. Soc.* **130**, 10187–10198 (2008).
45. Krenske, E. H. & Houk, K. N. Aromatic interactions as control elements in stereoselective organic reactions. *Acc. Chem. Res.* **46**, 979–989 (2013).
46. Wheeler, S. E. Understanding substituent effects in noncovalent interactions involving aromatic rings. *Acc. Chem. Res.* **46**, 1029–1038 (2013).
47. Wheeler, S. E. & Bloom, J. W. G. Toward a more complete understanding of noncovalent interactions involving aromatic rings. *J. Phys. Chem. A* **118**, 6133–6147 (2014).
48. Isidro-Llobet, A., Álvarez, M. & Albericio, F. Amino acid-protecting groups. *Chem. Rev.* **109**, 2455–2504 (2009).
49. Blaskovich, M. A. T. Unusual amino acids in medicinal chemistry. *J. Med. Chem.* **59**, 10807–10836 (2016).
50. Agostini, F. et al. Biocatalysis with unnatural amino acids: enzymology meets xenobiology. *Angew. Chem. Int. Ed.* **56**, 9680–9703 (2017).
51. Drienovská, I. & Roelfes, G. Expanding the enzyme universe with genetically encoded unnatural amino acids. *Nat. Catal.* **3**, 193–202 (2020).

Methods

General. For the ^{1}H NMR, ^{13}C NMR spectra and HPLC traces of compounds in this Article, details of synthetic procedures and details of the computational study, see the Supplementary Information.

General procedure for ruthenium-catalysed 1,3-nitrogen shift. To a Schlenk tube was added the azanyl ester (1 equiv.), K_2CO_3 (3 equiv.) and the ruthenium catalyst (1–2 mol% of Λ-**RuDMP** or 2–10 mol% of Λ-**RuH**). The tube was evacuated and backfilled three times with nitrogen. Dichloromethane (0.05 M) was added, and the tube was sealed. The reaction mixture was stirred at room temperature (25 °C) for 16 h. After completion, the reaction was quenched by a mixture of brine and hydrochloric acid, and subsequently extracted with EtOAc. The combined organic layer was dried and concentrated under reduced pressure, and the residue was then purified by column chromatography on silica gel using a mixture of EtOAc and *n*-hexane (with 0.1% trifluoroacetic acid as the additive) to obtain non-racemic α-amino acids **2**–**36** and **38**–**42**.

General procedure for iron-catalysed 1,3-nitrogen shift. To a Schlenk tube was added the azanyl ester (1 equiv.), K_2CO_3 (3 equiv.) and (*R*,*R*)-[$FeCl_2$(**BIP**)] (8–15 mol%). 1,1,2,2-Tetrachloroethane (0.1 M) was added, and the mixture was degassed via two freeze–pump–thaw cycles. The tube was sealed, and the reaction mixture was stirred at 0 °C for 40 h or at room temperature (25 °C) for 16 h. After completion, the reaction was quenched by a mixture of brine and hydrochloric acid, and subsequently extracted with EtOAc. The combined organic layer was dried and then concentrated under reduced pressure, and the residue was purified by column chromatography on silica gel using a mixture of EtOAc and *n*-hexane (with 0.1% trifluoroacetic acid as the additive) to obtain the non-racemic α-amino acids **43**–**53**.

Data availability

All relevant data supporting the findings of this study, including experimental procedures and compound characterization, NMR and HPLC are available within the article and its Supplementary Information.

Acknowledgements

This project has received funding from the European Research Council (ERC) under the European Union's Horizon 2020 research and innovation programme (grant agreement number 883212). Funding was also provided by the Deutsche Forschungsgemeinschaft (Me 1805/15-1). S.C. thanks Oberlin College for financial support. DFT calculations were performed using the SCIURus, the Oberlin College HPC cluster (NSF MRI 1427949), and the startup allocations awarded by Extreme Science and Engineering Discovery Environment (XSEDE TG-CHE200100).

Author contributions

E.M. and S.C. wrote the manuscript. E.M. and C.-X.Y. conceived the project and devised the experiments for the ruthenium catalysis. E.M. and X.S. devised the experiments for the iron catalysis. C.-X.Y. carried out the initial experiments and developed the ruthenium catalysis. X.S. developed the iron catalysis. S.C. performed the DFT calculations.

Competing interests

E.M., C.-X.Y. and X.S. are named inventors on a European patent application (EP22163544.4) filed by the University of Marburg on the synthesis of α-amino acids via 1,3-nitrogen migration. S.C. declares no competing interests.

Additional information

Supplementary information The online version contains supplementary material available at https://doi.org/10.1038/s41557-022-00895-3.

Correspondence and requests for materials should be addressed to Shuming Chen or Eric Meggers.

Peer review information *Nature Chemistry* thanks Trevor Hamlin and the other, anonymous, reviewer(s) for their contribution to the peer review of this work.

Reprints and permissions information is available at www.nature.com/reprints.